Cell dynamics model of droplet formation in polymer-dispersed liquid crystals

P. I. C. Teixeira and B. M. Mulder
FOM–Institute for Atomic and Molecular Physics,
Kruislaan 407, NL-1098 SJ Amsterdam, The Netherlands
(Received 12 April 1995)

We present a model for the dynamics of formation and morphology of polymer-dispersed liquid crystals (PDLCs). This incorporates, in a simplified manner, all the key physical ingredients of the actual fabrication process, viz., polymerization and gelation, phase separation, and growth and stabilization of a spatially inhomogeneous structure. We model phase separation of the initial pre-PDLC mixture into monomer- and liquid-crystal (LC)-rich phases by the cell dynamics systems (CDS) method of Oono and Puri [Phys. Rev. Lett. **58**, 836 (1987); Phys. Rev. A **38**, 434 (1988); **38**, 1542 (1988)]. Gelation at the expense of monomers is described by an auxiliary field (the phase field), which also obeys a CDS equation for the conserved-order-parameter case. Growth is assumed to occur at the gel surface. Finally, structure stabilization is achieved by the inclusion of a nonlocal term that mimics the effect of the long-range interaction responsible for gel cohesion. We have performed detailed numerical calculations on a two-dimensional system for an initial composition of 30% LC plus 70% monomer. A pattern of LC-rich droplets is found to develop that is stable as $t \to \infty$, where t is time. Moreover, the droplet size distribution exhibits a very sharp peak, in agreement with observations on real PDLCs.

PACS number(s): 61.41+e, 64.75+g, 81.20.Ti

I. INTRODUCTION

Polymer-dispersed liquid crystals (PDLCs) are dispersions of liquid-crystal rich droplets in a polymer matrix [1,2]. These can be prepared by a variety of techniques, all involving the (macroscopically) incomplete phase separation ("microphase separation") of an initially homogeneous mixture, which have been reviewed by West [3]. We are concerned with polymerization-induced phase separation (PIPS), which is illustrated schematically in Fig. 1. Here the liquid crystal (LC) is dissolved in the polymer precursor (prepolymer), which is then polymerized by addition of chemical activators, or irradiation with ultra-violet light or electron beams (see, e.g., [4] and references therein). The resulting change in the chemical potential of the solvent leads to phase separation of the LC via droplet nucleation. The mixture continues to phase separate until gelation of the polymer halts droplet growth. In the remainder of this introduction we shall restrict our attention to systems containing only the simplest type of LC, i.e., a nematic LC, thus effectively ignoring more recent realizations that make use of cholesteric or smectic liquid crystals [4].

PDLCs are a subject of considerable interest, both fundamental and applied. On the fundamental side, they raise challenging questions addressing very basic aspects of LC research, such as the dynamics of phase separation, ordering and structure selection, as well as finite size and surface effects at equilibrium. The popularity they enjoy among technologists, however, is due to their potentially applicable electro-optic properties. By matching the refractive index of the polymer and the ordinary refractive index of the LC, PDLC films can be switched from a translucent "off" state to a transparent "on" state by application of an electric field. In the field-off state, the director field inside each droplet is determined by the balance between nematic elasticity and surface anchoring; its orientation varies randomly from droplet to droplet, hence the film scatters light strongly and is opaque. If an electric field is applied perpendicular to the film, the director will align along the field direction and for normal light incidence the film becomes transparent [5]. Unlike conventional LC displays, these films are flexible and very easy to prepare, since no orienting glass plates, and hence

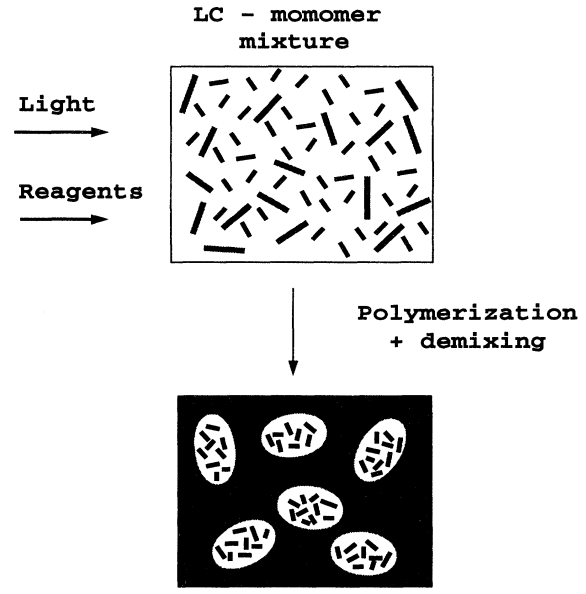

FIG. 1. The making of a PDLC by PIPS.

 ©1996 The American Physical Society

no complex surface treatments, are required. In addition, their light transmittance is much higher than that of the more conventional twisted- or supertwisted-nematic devices, owing to the absence of polarizers [6]. Some potential applications are switchable windows, display devices, infrared shutters, angular-discriminating filters, thermo-electro-optic switches, memories, gas flow sensors, optical sensors, and optical gratings [4].

Morphology, and in particular droplet size and density, has a major influence on the optoelectronic response of these materials and on the scattering efficiency of their films [7,8], which is maximized when the droplet size is on the order of the wavelength of light. Both the threshold voltage and the switching speed of the resulting display decrease with increasing droplet size [4]. Although much empirical knowledge has been gathered on the fabrication of PDLCs, a detailed understanding of the underlying physical mechanisms leading to specific properties is still lacking.

Palffy-Muhoray and co-workers [9–11] have applied the (linearized) Cahn-Hilliard theory of spinodal decomposition [12–15] to PDLCs. While this type of analysis yields information on relevant length scales and their time evolution in the early stages of phase separation, it cannot perforce reveal anything about the late-time behavior, or the spatial organization, of the system.

Using purely empirical arguments, Smith and coworkers [16–18] have been able to extract information on important aspects of PDLC morphology, such as the relationship between droplet diameter and droplet number density, and the fractional amount α of LC contained in droplets. The quantity α was later related to solubility parameters in the context of a thermodynamic treatment [19] based on the Flory-Huggins theory of polymer mixtures [20]. The nematic character of the LC is neglected throughout and a droplet structure is assumed as a starting point rather than derived.

More recently, Lin and Taylor [21] have developed a mean-field theory of multifunctional polymerization and gelation. Its application to PDLCs describes phase separation as a consequence of the rise in the upper critical solution temperature [22] due to the increasing degree of polymerization. In contrast to the process of phase separation by thermal quench, in which the operating point on the phase diagram descends vertically into the two-phase region, phase separation due to polymerization is represented as a stationary point on the phase diagram, which then becomes engulfed by the upward moving spinodal curve. Flory-Huggins theory is again used for the thermodynamics. A similar approach has been adopted by Hirai and co-workers [23,24], who, however, treat the nematic LC explicitly.

The earliest statistical mechanical model incorporating both phase separation and gelation is that of Coniglio, Stanley, and Klein [25,26]. It consists of a lattice of binary occupation variables representing monomers and solvent molecules, with the key feature that two nearest-neighbor monomers can interact with two different energies, chosen according to a given probability. These correspond to either the usual van der Waals interaction or a (much larger) chemical bond energy. Theoretical work on this model has concentrated on the (equilibrium) phase diagram, which exhibits, in addition to the usual miscibility gap of ordinary fluid mixtures, a line of sol-gel transitions. A recent Monte Carlo simulation [27] has revealed that, if the probability of forming a strong bond is large enough, the system becomes "pinned," i.e., further growth of phase-separating domains is arrested by the gel network. Yet this "microphase separated" state is a nonequilibrium one, expected to decay if the simulation is carried to longer "times," on account of the fact that bond formation is reversible. No results have as yet been reported for a modification of this model to include unbreakable bonds between monomers [28].

A continuum version of the Coniglio-Stanley-Klein model [29] has been proposed by Sciortino and co-workers [30]. Phase separation and gelation are modeled by time-dependent Ginzburg-Landau equations for the conserved and nonconserved order-parameter cases, respectively [31]. The coupling between the two phenomena is accomplished by letting monomer mobility depend on gel concentration and the gelation threshold depend on monomer concentration. Although this theory successfully introduces irreversibility, it treats gelation as an equilibrium process governed by a "free energy," which is somewhat questionable.

In this paper we present a model for the dynamics of formation and morphology of PDLCs that captures, in a simplified manner, most of the essential physics of the actual fabrication process, viz., polymerization and gelation, phase separation, and growth and stabilization of a spatially inhomogeneous structure. In Sec. II we start by summarizing our idealization of PDLC formation dynamics. We then introduce our dynamical model and discuss its different ingredients. In Sec. III results are presented for the monomer and gel concentration patterns, as well as for the circularly averaged gel structure factor, droplet size distribution, and mean droplet size, as a function of time. We justify our choice of model parameters and show that our data are in qualitative agreement with observations on real PDLC systems. Finally, in Sec. IV we conclude by summarizing our results and discussing possible improvements to our model, as well as future directions of research.

II. THEORY

A. Primer of model building

Consider a three-component system consisting of a nematic LC, "monomer," and "gelled polymer." At this rather early stage we do not introduce any radicals or initiators as occur in real systems. Although the final morphology obviously depends on *general* features of the fabrication process such as the rate of polymerization, intensity and duration of irradiation, or cure temperature, its detailed chemistry might not be too relevant. Moreover, we shall also neglect the nematic character of the LC component, consideration of which should not change our results substantially. Indeed, in the (mean-field-like) type of theory we are using, nematic order-

ing occurs when the (local) concentration of the nematic component exceeds a certain threshold. Since this only happens in regions where phase separation is already well advanced, it is unlikely to influence the corresponding dynamics. Inclusion of the nematic effect would, of course, be crucial for a realistic modeling of the optical properties of PDLCs.

We start by assuming that the incompressibility condition is satisfied, viz.,

$$c_{\mathrm{LC}} + c_m + c_g = 1, \tag{1}$$

where c_{LC}, c_m, and c_g are the concentrations of the LC, monomer, and gel, respectively. We emphasize that this need not be true of a real pre-PDLC mixture, in which case a more sophisticated treatment would be called for. One possibility would be to add "voids" as an additional, noninteracting, component, the chemical potential of which would be proportional to the pressure [32]. As a first approach, however, we restrict ourselves to the simplest case.

We begin by giving a brief summary of PDLC formation as we idealize it. At time $t = 0^+$, i.e., immediately after polymerization has been initiated, our mixture consists predominantly of LC and monomer (typically, $c_{\mathrm{LC}} \ll c_m$) and a small amount of gel ($c_g \ll 1$). Now as "gelation" (which in this model is not distinct from polymerization) proceeds, c_g will increase at the expense of c_m, while c_{LC} remains constant (since the LC does not take part in the chemical reaction). Hence c_{LC} and $c_m + c_g$ are conserved, but not c_m or c_g individually. Note that the incompressibility relation, Eq. (1), implies that there are only *two* independent concentration variables (e.g., c_m and c_g). As the monomer is depleted, the mixture, initially in the one-phase region of its phase diagram, is driven into the two-phase region and begins to phase separate, since the LC and gel become less and less miscible. At the same time, an underlying gel network is formed, which eventually arrests growth of LC- and monomer-rich domains. We therefore expect that, for sufficiently low LC concentrations and appropriate gelation rates, the final product will consist of a dispersion of LC-rich droplets in a gel matrix. We expect *two* length scales to appear in the problem, one associated with phase separation (average size and/or separation of domains) and one associated with the finer network structure due to gelation. This is similar to what is observed in gelatin-water-methanol mixtures [33,34]. Likewise, the above phenomena are expected to occur on two (potentially very) different time scales. One final difficulty concerns the stabilization of a microphase-separated, spatially inhomogeneous, structure.

Perhaps the simplest model conceivable is one in which phase separation is described by the usual spinodal decomposition formalism [31], whereas polymerization and gelation are modeled by a modified version of diffusion-limited aggregation [35]. The latter amounts to assuming a "chemically naive," "contact" chemical reaction mechanism: monomers are allowed to diffuse until they encounter a gel site, where they stick with a given probability [36]. Diffusion of gel particles is never allowed.

Simple and attractive as this model might be, it nevertheless proves physically unreasonable. Indeed, *global* conservation (i.e., conservation of the total amount of LC plus monomer plus gel) introduces spatial correlations in the concentration fields, which are neglected in this approach: depletion of a particular chemical species due to chemical reaction at a certain location is effectively decoupled from the dynamics of the corresponding concentration field. This, combined with the fact that the gel is not allowed to relax dynamically in order to accommodate spatial inhomogeneities in a self-consistent manner, leads to unphysical results, such as unbounded negative concentrations. Put more simply, phase separation has its own dynamics; this need not be the same as that of a naive chemical reaction–diffusion-limited aggregation model, which is characterized by wholly different time and length scales.

Clearly, the difficulties described above originate in the attempt to unite, in a single theoretical scheme, three fundamentally different phenomena currently described by unmarriageable models, i.e., polymerization, phase separation, and structure growth. Of these, polymerization is intrinsically nonconserving, since it involves mutation of one chemical species into another. Phase separation, on the other hand, is intrinsically conserving, since it only concerns the spatial redistribution of matter. Finally, structure growth requires tracking a surface in space [37], a task to which a formulation in terms of partial differential equations as is commonly employed in theories of phase separation [31] is particularly ill suited [38,39]. To overcome these hurdles we resort to a phase field model.

B. A phase field model

Phase field models were originally invented to study solidification [40], having since been applied to other growth processes (see, e.g., [41,42] and references therein). The phase field is an auxiliary function of time and space, satisfying some appropriate equation. The interface is then *defined* as the set of contour lines corresponding to a particular value of the phase field. Thus we effectively replace a moving-boundary (Stefan) problem by a simpler fixed-boundary problem involving one additional equation. No distinction is made between the different phases and their interfaces, hence the whole domain can be treated in the same way numerically. Moreover, this approach allows the computation of realistically complicated interfacial structures whose connectedness changes in time, and we believe it to be particularly suited to our problem, which combines phase separation and structure growth.

It remains to derive the appropriate equations for the system. Rather than using the conventional formulation of ordering dynamics in terms of partial differential equations, we opted for the computationally efficient cell dynamics systems (CDS) method of Oono and Puri [43–45], where space is assumed discrete from the outset and divided into "cells." Modeling then consists of two steps: (i) modeling of each cell, and (ii) connecting cells. The

first step is essentially the calculation of the thermodynamic force that drives the order parameter within that cell to the value pertaining to either of the phases in equilibrium and away from the single unstable state. Here the need to define a nonequilibrium free energy is circumvented by introducing a map (i.e., an injection of the set of real numbers, where the order parameter takes values) with stable fixed points corresponding to the two coexisting phases and an unstable fixed point corresponding to the unstable one-phase state. Next, cells are connected to take cooperative interactions into account: the nonlocal driving force for order parameter change in a given cell is taken to be proportional to the difference between the value of the order parameter in that cell and a suitably defined average of its values in neighboring cells. In addition, in the conserved-order-parameter case that concerns us here, a correction must be applied to ensure conservation. For details of the method we refer the reader to the original publications [43–45].

We consider a two-dimensional (2D) system for simplicity. Our modeling of PDLCs then proceeds as follows.

(i) Following Keblinski and co-workers [42], we introduce two coupled fields ψ and ϕ, the former describing the field causing the growth and the latter describing the presence ($\phi > 0.5$) or absence ($\phi < 0.5$) of gel. The interface between gel and nongel is thus defined as the contour line $\phi(x,y) = 0.5$. Note that our fields take values in the interval $(0,1)$ instead of the more common $(-1,+1)$. Hence ψ is the monomer concentration.

(ii) We model phase separation in the primordial LC-monomer mixture using the CDS method. ϕ is also evolved according to the conserved-order-parameter version of the CDS method, reflecting the reasonable assumption that no growth can occur in the absence of monomers. Furthermore, we couple the two fields in such a way that the gel grows at the expense of the monomer, by inclusion of a sink term in the equation for ψ, and of a source term in that for ϕ. More precisely, we require that our fields satisfy

$$\psi(\mathbf{x},t+1) = \mathcal{F}_\psi[\psi(\mathbf{x},t)] - \langle\langle \mathcal{F}_\psi[\psi(\mathbf{x},t)] - \psi(\mathbf{x},t)\rangle\rangle - I(\mathbf{x},t), \quad (2)$$

$$\phi(\mathbf{x},t+1) = \mathcal{F}_\phi[\phi(\mathbf{x},t)] - \langle\langle \mathcal{F}_\phi[\phi(\mathbf{x},t)] - \phi(\mathbf{x},t)\rangle\rangle + \alpha I(\mathbf{x},t) - \xi\left[\phi(\mathbf{x},t) - \overline{\phi}(t)\right], \quad (3)$$

with

$$\mathcal{F}_\psi[\psi(\mathbf{x},t)] = f(\psi(\mathbf{x},t)) + D_\psi[\langle\langle\psi(\mathbf{x})\rangle\rangle - \psi(\mathbf{x},t)], \quad (4)$$

$$\mathcal{F}_\phi[\phi(\mathbf{x},t)] = f(\phi(\mathbf{x},t)) + D_\phi[\langle\langle\phi(\mathbf{x})\rangle\rangle - \phi(\mathbf{x},t)]. \quad (5)$$

$\langle\langle * \rangle\rangle - *$ is the isotropized discrete "Laplacian" on the 2D square lattice [44],

$$\langle\langle *(\mathbf{x},t)\rangle\rangle = \frac{1}{6}\sum_{\mathrm{NN}} *(\mathbf{x},t) + \frac{1}{12}\sum_{\mathrm{NNN}} *(\mathbf{x},t), \quad (6)$$

where NN and NNN denote nearest and next-nearest neighbors, respectively. Moreover, we have the following.

(a) $I(\mathbf{x},t) > 0$ is an interaction term leading to growth of gel and depletion of monomer such that the quantity $\phi + \alpha\psi$ is globally conserved. α is the "exchange rate" between fields ψ and ϕ; we set $\alpha = 1$ in all our calculations, in which case it is legitimate to identify ϕ with the gel concentration. We choose $I(\mathbf{x},t)$ to be of the form

$$I(\mathbf{x},t) = c\,\psi(\mathbf{x},t)|\nabla\phi(\mathbf{x},t)|, \quad (7)$$

where c is a positive constant. With this choice of interaction term, growth occurs at the gel surface ($|\nabla\phi| \neq 0$) whenever monomers are present ($\psi \neq 0$). We approximated the gradient in Eq. (7) by the usual space-centered difference formula [46].

(b) For $f(x)$ we introduce a variant of the tanh map, with stable fixed points 0 and 1, unstable fixed point 0.5, viz.,

$$f(x) = \frac{1}{2}\left\{1 + A\tanh\left[\tanh^{-1}\left(\frac{1}{A}\right)(2x-1)\right]\right\}, \quad (8)$$

with $A = 1.3$ as in preceding work [43,44].

(c) The (nonlocal) term multiplying ξ in Eq. (3) stabilizes the pattern at its instantaneous composition [47–49], thus freezing late-stage growth. This will be discussed in more detail below. $\overline{\phi}(t)$ is the spatially averaged gel concentration, given by Eq. (14).

(iii) The choice of initial conditions is motivated by our interest in modeling chain polymerization, an intrinsically inhomogeneous process [50] used in the fabrication of real PDLCs. A calculation is started by assigning values $\psi_{i,j}(t=0) = 0$ and $\phi_{i,j}(t=0) = 1$ to a fraction g of (randomly chosen) lattice sites and $\psi_{i,j}(t=0) = \psi_0$ and $\phi_{i,j}(t=0) = 0$ to all other sites, where ψ_0 is the initial concentration of monomer and we have defined $\psi_{i,j}(t) \equiv \psi(x_i, y_j, t)$ and $\phi_{i,j}(t) \equiv \phi(x_i, y_j, t)$, with $x_i = (i-1)h$ and $y_j = (j-1)h$ ($i = 1,2,\ldots,N$; $j = 1,2,\ldots,N$, h is the lattice spacing, taken as the unit of length). Nongel sites are then biased so that the average monomer concentration is ψ_0 (because $g \ll 1$, this correction is usually quite small). Equations (2) and (3) are then advanced in time.

The nonlocal term multiplying ξ in Eq. (3) was first introduced in a CDS model of microphase separation in block copolymer mixtures by Oono and co-workers [47–49], in the context of which it can be shown from dimensional arguments that $\xi \propto l^{-2}$ (l being the chain length). Things become much more transparent if we consider the corresponding partial differential equation for ϕ [51],

$$\frac{\partial\phi(\mathbf{x},t)}{\partial t} = \nabla^2[-\phi(\mathbf{x},t) + \phi^3(\mathbf{x},t) - \nabla^2\phi(\mathbf{x},t)] - \xi[\phi(\mathbf{x},t) - \overline{\phi}(t)], \quad (9)$$

where we have dropped the chemical reaction term. This is legitimate in view of the fact that stabilization prevails only after all chemistry has stopped due to exhaustion of monomer (see Sec. III). Now it is easily seen that Eq. (9) can be derived from a free energy functional containing, besides the usual short-range term F_{SR}, a contribution from a long-range interaction

$$F = F_{\rm SR} + F_{\rm LR}$$
$$= \int d\mathbf{x} \left[-\frac{1}{2}\phi^2(\mathbf{x},t) + \frac{1}{4}\phi^4(\mathbf{x},t) + \frac{1}{2}\left[\nabla\phi(\mathbf{x},t)\right]^2 \right]$$
$$+ \xi \int d\mathbf{x} d\mathbf{x}' \left[\phi(\mathbf{x},t) - \overline{\phi}(t)\right]$$
$$\times G(\mathbf{x}-\mathbf{x}') \left[\phi(\mathbf{x}',t) - \overline{\phi}(t)\right], \quad (10)$$

where $G(\mathbf{x}-\mathbf{x}')$ is the Green's function for Laplace's equation, satisfying $\nabla^2 G(\mathbf{x}-\mathbf{x}') = -\delta(\mathbf{x}-\mathbf{x}')$. In block copolymer mixtures the long-range contribution originates from the fact that macroscopic phase separation is inhibited by connectivity, which imposes a penalty on long-range fluctuations of the composition [52,53]. Furthermore, Eq. (10) is equivalent to the model proposed by Sagui and Desai to describe amphiphilic films [54] in the limit of infinite film thickness L, for which their $g(\mathbf{x}-\mathbf{x}')$ and our $G(\mathbf{x}-\mathbf{x}')$ coincide. In this case, for an appropriate composition a droplet pattern will develop that freezes in a monodisperse configuration at late times [55]. The linear stability of periodic, steady-state solutions to Eq. (9) in one-dimension was first investigated by Bahiana and Oono [49] using a simplified form for $F_{\rm SR}$ and by Liu and Goldenfeld [56]. More recently, Glotzer and Coniglio have analyzed Eq. (9) in the limit of infinite-order-parameter dimension n [57] and found a microphase-separated state if $0 < \xi < \frac{1}{4}$, in agreement with Liu and Goldenfeld's 1D result [58].

The selection of a length scale can be more easily understood by writing the long-range part of the free energy $F_{\rm LR}$ in terms of the Fourier components of ϕ,

$$F_{\rm LR} = \xi \sum_{\mathbf{k}} \frac{|\delta\phi_{\mathbf{k}}(t)|^2}{k^2}, \quad (11)$$

$$\phi(\mathbf{x},t) - \overline{\phi}(t) = \sum_{\mathbf{k}} \delta\phi_{\mathbf{k}}(t) e^{-i\mathbf{k}\cdot\mathbf{x}}, \quad (12)$$

which penalizes small-k (long-wavelength) fluctuations ($k = |\mathbf{k}|$). Now Eq. (11) is exactly that introduced by de Gennes in his treatment of the effect of cross links on a mixture of polymers [59], where use was made of an electrostatic analogy. Studies of the dynamics of phase separation in block copolymer systems including this term (albeit restricted to the linear regime) have been reviewed by Daoud [60]. Finally, we note that Eq. (9) has also been proposed to study phase separation in chemically reactive mixtures [11,61–63].

III. RESULTS

We have integrated Eqs. (2)–(5) with initial conditions as described in the preceding section and periodic boundary conditions, on a square lattice of size $N^2 = 64 \times 64$, for $\psi_0 = 0.7$, $g = 0.01$, $A = 1.3$, $D_\psi = D_\phi = 0.5$, $c = 1.0$, and $\xi = 0.01$. ψ_0 is chosen so as to be in the droplet-forming region of the phase diagram of a binary mixture; it lies above the site percolation threshold for the square lattice ($\approx 0.592\,75$ [64]) and corresponds to $\Phi = 2\phi - 1 = 0.4$, where $\Phi \in (-1,1)$ is the more usual order parameter of spinodal decomposition studies. This

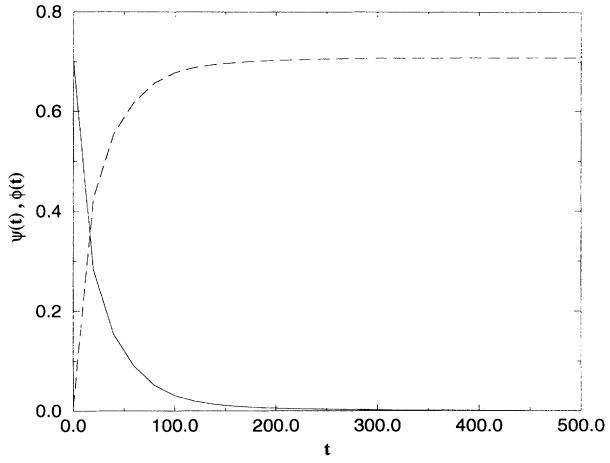

FIG. 2. Spatially averaged monomer (solid line) and gel (dashed line) concentrations vs time, for $\psi_0 = 0.7$, $g = 0.01$, $D_\psi = D_\phi = 0.5$, $c = 1.0$, and $\xi = 0.01$.

effectively puts us in the hexagonal phase of Sagui and Desai's model (see Fig. 1 in [54]), which should further enforce monodispersity [55]. Moreover, it is consistent with the experimental requirement that LC concentrations should be below $\sim$ 53% volume, above which an inverted phase of polymer droplets in a LC matrix ("polymer ball") is found [17,65].

The volume fraction of initial gel "seeds," g must be small enough that it does not lead to a uniform gel. On the other hand, ξ will fail to arrest phase separation if too small, but prevent it completely if too large. A is as in preceding studies [44] and c has been chosen for computational convenience, pending a more realistic description of the chemical processes involved.

Taking $D_\psi = D_\phi$ may appear puzzling at first sight, given the fundamentally different natures of monomer

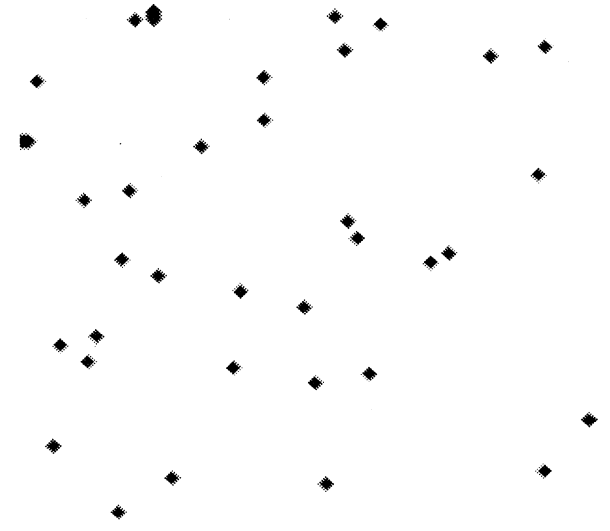

FIG. 3. Gel concentration at $t = 0$, for the same system as in Fig. 2.

and gel. In our experience, however, changing these quantities only accelerates or decelerates the dynamics, but does not alter it qualitatively. This is supported by a study of the Ginzburg-Landau equation with a concentration-dependent mobility [66].

Figure 2 shows the spatially averaged concentrations, defined as

$$\overline{\psi}(t) = \frac{1}{N^2} \sum_{i,j=1}^{N} \psi_{i,j}(t), \tag{13}$$

$$\overline{\phi}(t) = \frac{1}{N^2} \sum_{i,j=1}^{N} \phi_{i,j}(t), \tag{14}$$

for a typical run. Essentially all the chemistry takes place in the first ~ 250 time steps, after which concentrations

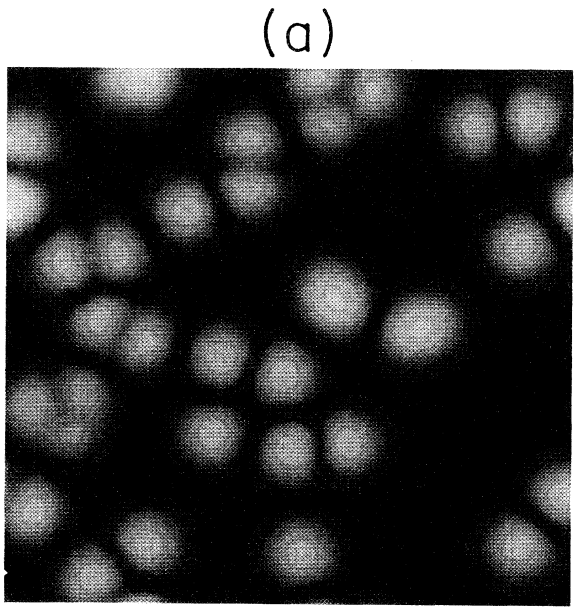

FIG. 4. (a) Monomer and (b) gel concentrations for the same system as in Fig. 3, but at $t = 10$.

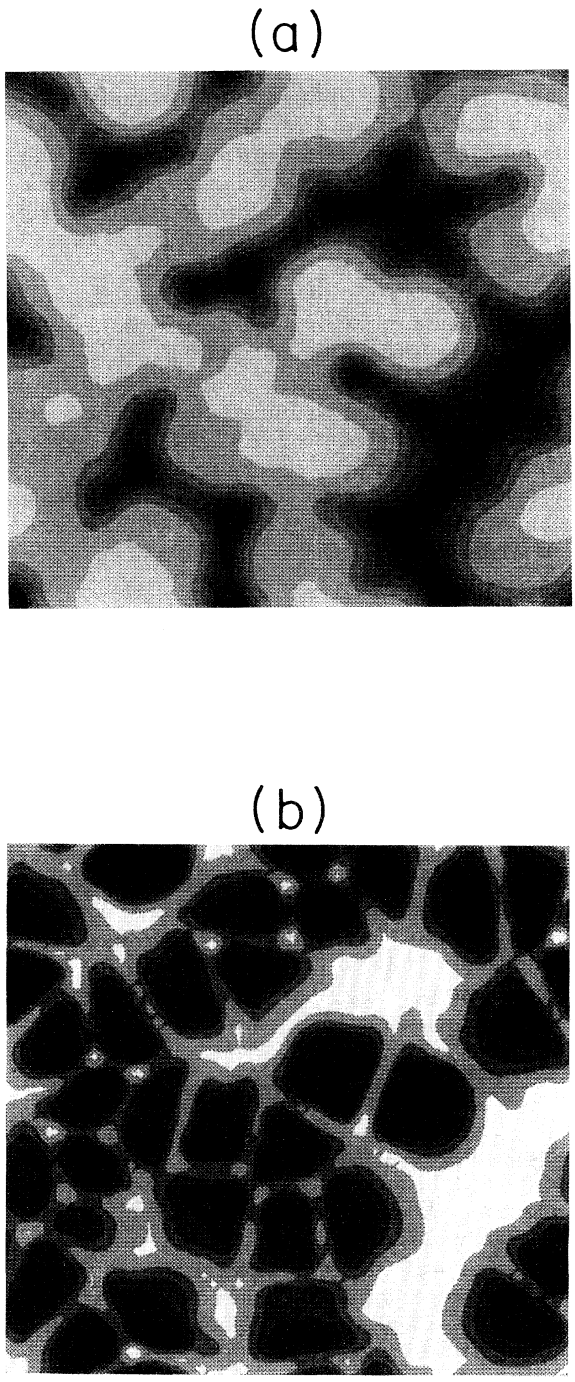

FIG. 5. Same as Fig. 4, but at $t = 50$.

take on their asymptotic values corresponding to total exhaustion of monomer.

Figures 3–10 are snapshots of the system for times $t = 0$ to $t = 5 \times 10^4$ (measured in number of lattice updates). In all contour plots, the depth of shading is proportional to the height of the function plotted. Figure 3 shows the initial condition for ϕ, i.e., the gel seeds at $t = 0$. The growth of gel from these initial inhomogeneities [cf. Eq. (7)] is shown in Figs. 4–6; note the complementarity of (a) ψ and (b) ϕ. The gel network then percolates and consequently the gel-poor region fragments into a number of "holes" (Fig. 6). At this stage, practically all of the monomer has been exhausted but the incipient gel still contains vast regions of fairly low ϕ (Fig. 7), within which gel-poor (LC-rich) droplets nucleate (Figs. 7 and 8). At later times, black is predominantly gel (maximum concentration $\sim 85\%$), while white is predominantly LC (maximum concentration $\sim 90\%$). All action seems to cease after $t \sim 2 \times 10^4$.

All results presented henceforth are averages over ten runs. We computed the 2D gel structure factor, defined by

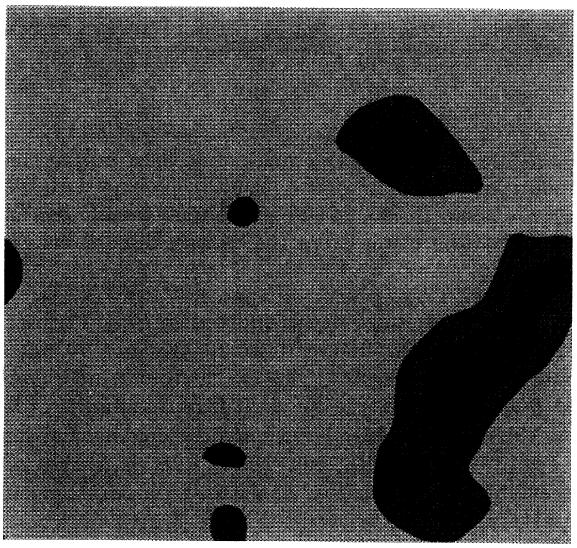

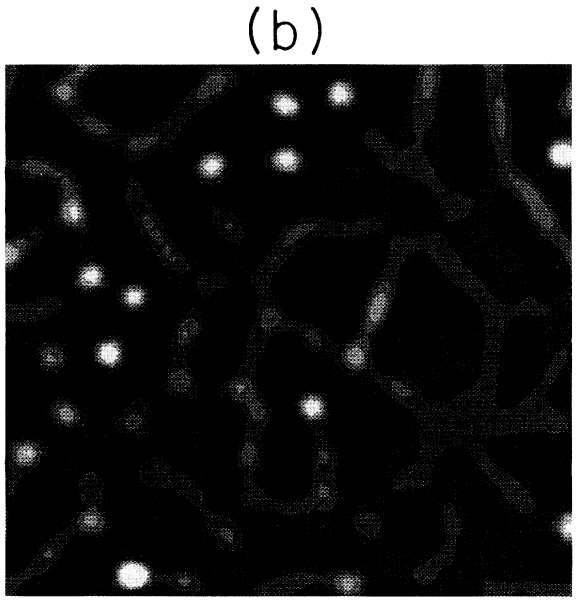

FIG. 6. Same as Fig. 4, but at $t = 100$.

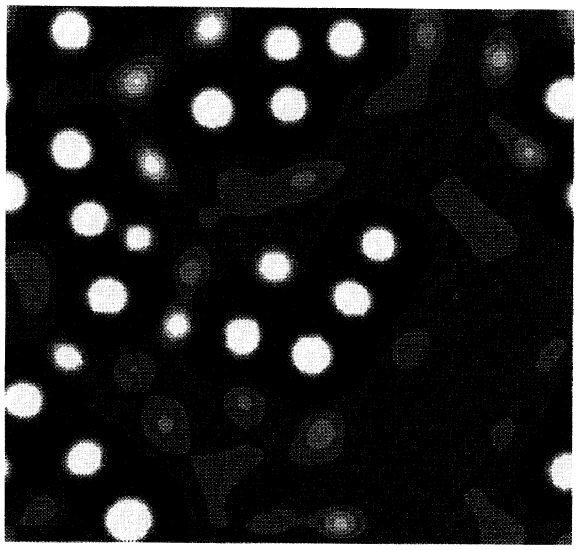

FIG. 7. Gel concentration at $t = 250$, for the same system as in the preceding figures.

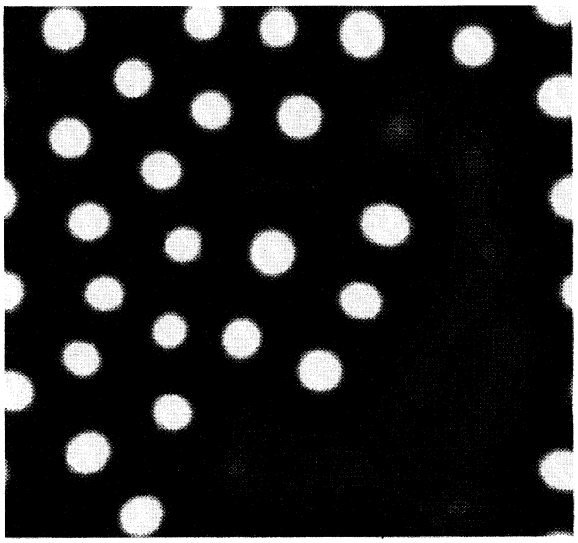

FIG. 8. Same as Fig. 7, but at $t = 1000$.

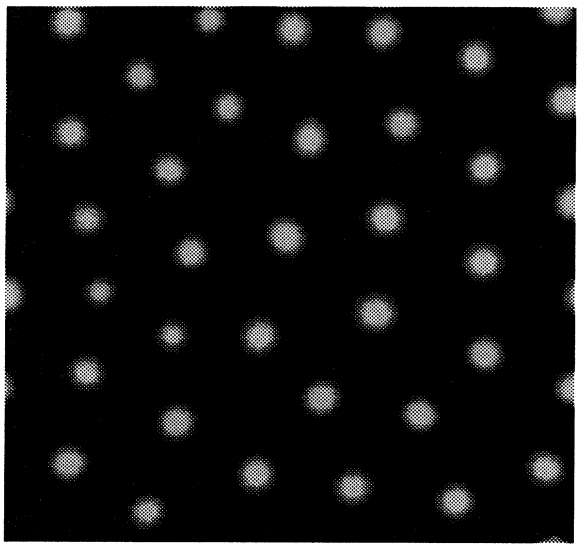

FIG. 9. Same as Fig. 7, but at $t = 5000$.

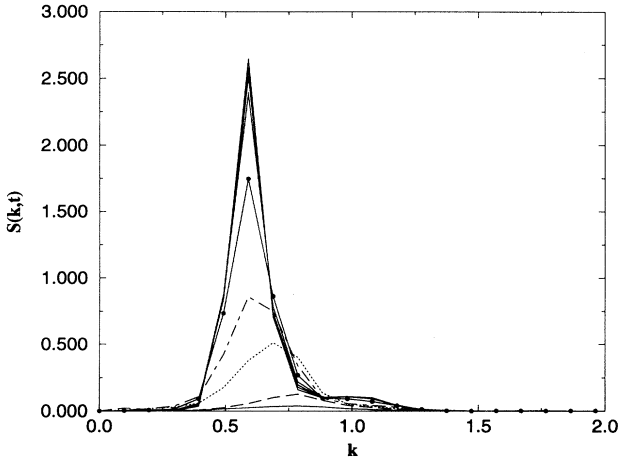

FIG. 11. Circularly averaged gel structure factor at $t = 100$ (solid line); $t = 200$ (dashed line); $t = 500$ (dotted line); $t = 1000$ (dot-dashed line); $t = 2000$ (solid line with filled circles); $t = 5000$, 10 000, 20 000, and 50 000 (remaining solid lines, from bottom to top). See the text for discussion.

$$S(\mathbf{k},t) = \left\langle \frac{1}{N^2} \left| \sum_{i,j} [\phi_{i,j}(t) - \overline{\phi}(t)]\, e^{i\mathbf{k}\cdot(i,j)} \right|^2 \right\rangle, \quad (15)$$

where $\mathbf{k} = (2\pi/N)(m\hat{\mathbf{e}}_1 + n\hat{\mathbf{e}}_2)$, $m,n = -(N/2) + 1,\ldots,N/2$, and the angular brackets denote averaging over initial conditions. The circularly averaged structure factor is then

$$S(k,t) = \sum_{\mathbf{k}} S(\mathbf{k},t) \Big/ \sum_{\mathbf{k}} 1, \quad (16)$$

with $k = 2\pi n/N$, $n = 0,1,2,\ldots,N$, and the sum $\sum_{\mathbf{k}}$ is over a circular shell defined by $n - \frac{1}{2} \leq |\mathbf{k}|N/(2\pi) \leq n + \frac{1}{2}$. This latter quantity is plotted in Fig. 11 for $t = 100$, 200, 500, 1000, 5000, 10 000, 20 000, and 50 000. In the coarsening regime ($t \lesssim 2000$), the peak increases in height due to gel segregation and shifts to smaller values of k as the characteristic length scale increases [compare with Fig. 14(b) in [54]]. For $2000 \lesssim t \lesssim 20\,000$ only segregation, but no further growth of domains, occurs. The pattern is effectively frozen for $t \gtrsim 20\,000$.

In order to perform a droplet size analysis we started by "hardening" the pattern at time t by assigning to each lattice site (i,j) an "Ising spin variable" $s_{i,j}$ such that $s_{i,j} = 1$ if $\phi_{i,j} < 0.5$ and $s_{i,j} = 0$ otherwise. This allowed us to identify droplets of "nongel" (i.e., LC, since there is no monomer left) as clusters of 1's. These clus-

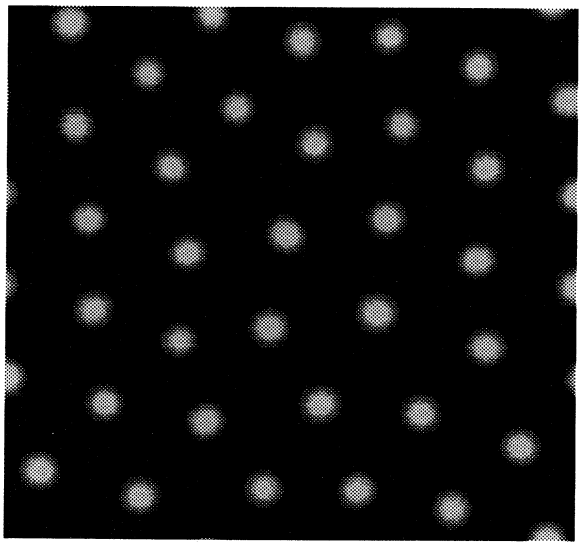

FIG. 10. Same as Fig. 7, but at $t = 50\,000$.

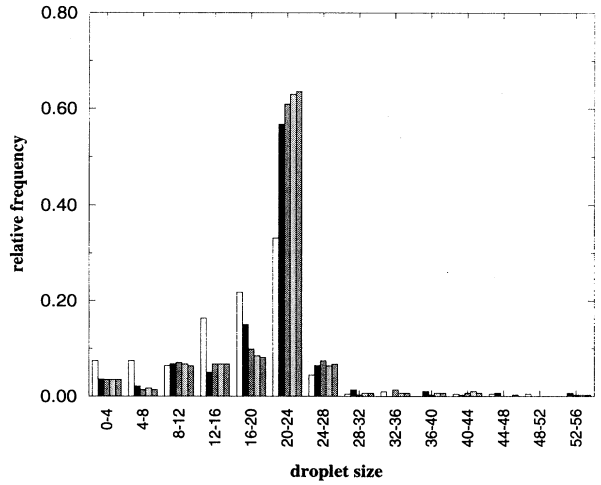

FIG. 12. Droplet size frequency histograms. From left to right: $t = 1000$, 5000, 10 000, 20 000, and 50 000. The corresponding mean droplet sizes and standard deviations are given in Table I.

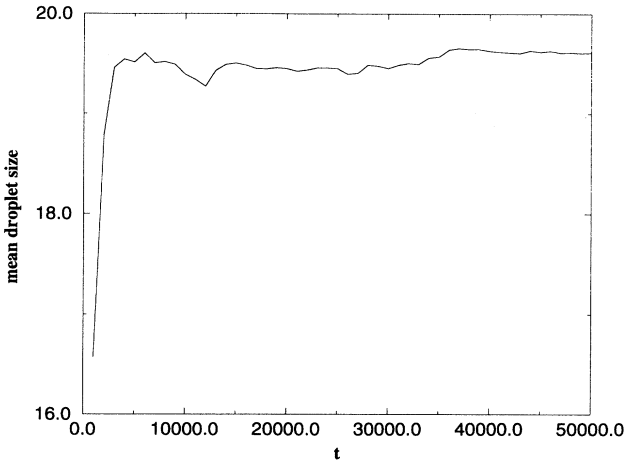

FIG. 13. Mean droplet size (number of sites per droplet) vs time, starting at $t = 1000$.

ters were then labeled and their size distribution found. Droplet size frequency histograms for $t = 1000$, 5000, 10 000, 20 000, and 50 000 are shown in Fig. 12. Sizes are given as number of spins per droplet and the bin width is 4. At the latest times shown (frozen pattern), more than 60% of all droplets have sizes between 20 and 24. In Fig. 13 we plot the mean droplet size as a function of time; note that it is constant on the scale of the standard deviation (not shown in the figure; see Table I).

TABLE I. Mean droplet sizes and standard deviations for the data in Fig. 15.

t	Mean droplet size	Standard deviation
1000	16.6	7.5
5000	19.6	6.9
10000	19.4	6.4
20000	19.5	6.5
50000	19.6	6.5

IV. CONCLUSION

We have developed what is perhaps the simplest model of PDLC formation incorporating phase separation, polymerization and gelation, and pattern formation. Results obtained for a suitable choice of model parameters are in agreement with observations on real PDLCs, for which tuning of the relevant physical parameters is also crucial. Our approach is based on the CDS method and is thus less computationally expensive than direct integration of nonlinear partial differential equations (typically the computational cost was less than 0.3 s per time step on a Silicon Graphics Indigo 3000 computer workstation).

We believe that our model captures most of the essential physics of the phenomena under study, albeit containing a fair degree of arbitrariness. Namely, we have the following.

(i) CDS models (as well as partial differential equation models) imply coarse graining on a not unambiguous mesoscopic length scale [44,67]. It is not obvious that the same coarse-graining procedure should be appropriate for LC-monomer and gel variables alike.

(ii) No distinction is made between polymerization and gelation, which are modeled in a simplified way allowing little control. Since the fabrication of real PDLCs relies rather heavily on being able to manipulate the chemistry, this is a shortcoming we need to remove in order to make closer contact with experiment.

(iii) A more realistic treatment of the gel structure including connectivity, and possibly also elasticity, would be most desirable.

(iv) Swelling of the gel by the LC-monomer, a potentially important effect when dealing with gel-solvent systems [20], has been neglected altogether.

Whether all, or any, of the above can be implemented in the present model, or whether they will necessitate a radical change of approach, remains unclear.

All results presented are for a two-dimensional, square system. We do not expect to see any significantly new physics by going to three dimensions, and thus the major investment of computational resources involved in such a step is, in our view, not justified at present. There might be a case, however, for switching to a triangular lattice. Recall that the motivation for the rather unconventional form of the Oono-Puri Laplacian, Eq. (6), is that it should yield as isotropic a pattern as possible, as well as good scaling of the corresponding structure factors [44]. Tomita [68] has shown that, of all 2D Laplacians including nearest and next-nearest neighbors on the square lattice, the Oono-Puri form yields optimal results. A similar analysis has been performed in three dimensions by Shinozaki and Oono [69]. It is easy to show that both the usual five-point approximation to the Laplacian and Oono and Puri's version are only isotropic to order k^2 [70], the difference between them being attributable to the magnitude of the correction terms at order k^4. By contrast, a Laplacian containing only nearest neighbors on a triangular lattice is isotropic to order k^4, due to the higher symmetry of the lattice. This is a well-known problem in lattice-gas [71] and lattice-Boltzmann [72] simulations, where isotropy is essential for recovering the correct hydrodynamic behavior.

ACKNOWLEDGMENTS

We thank Henk Boots and Hans Kloosterboer for sharing their knowledge on real PDLCs with us; Peter Bladon for writing the cluster labeling routine and for a critical reading of the manuscript; Pawel Keblinski for invaluable correspondence on phase field models; Maarten Hagen for help with the figures; Thierry Biben for advice on Fourier transforms; Frans Vitalis, Hans Verwer, Luís Trabucho, Irene Fonseca, and Peter Bates for assistance with the

more mathematical aspects of phase separation; Norbert Masbaum and Rashmi Desai for enlightening correspondence; and Toshihiro Kawakatsu and Sharon Glotzer for correspondence and for sending us copies of their work prior to publication. The work of the FOM Institute is part of the research program of FOM and is supported by the Nederlandse Organisatie voor Wetenschappelijk Onderzoek.

[1] J. W. Doane, N. A. Vaz, B.-G. Wu, and S. Žumer, Appl. Phys. Lett. **48**, 269 (1986).
[2] J. W. Doane, MRS Bull. **16**, 22 (1991).
[3] J. L. West, Mol. Cryst. Liq. Cryst. **157**, 427 (1988).
[4] H.-S. Kitzerow, Liq. Cryst. **16**, 1 (1994).
[5] Here it is assumed that the LC material has positive dielectric anisotropy. Reverse mode operation, where the PDLC is transparent in the "off" state and opaque in the "on" state, is also possible. This requires LCs with negative dielectric anisotropy and is relevant to some of the potential applications listed. See [4] for details.
[6] M. Schadt, Liq. Cryst. **14**, 73 (1993).
[7] B. G. Wu, J. L. West, and J. W. Doane, J. Appl. Phys. **62**, 3925 (1987).
[8] S. Žumer and J. W. Doane, Phys. Rev. A **34**, 3373 (1986).
[9] J. Y. Kim and P. Palffy-Muhoray, Mol. Cryst. Liq. Cryst. **203**, 93 (1991).
[10] J. Y. Kim, C. H. Cho, P. Palffy-Muhoray, M. Mustafa, and T. Kyu, Phys. Rev. Lett. **71**, 2232 (1993).
[11] P. Palffy-Muhoray (private communication).
[12] J. W. Cahn and J. E. Hilliard, J. Chem. Phys. **28**, 258 (1958).
[13] J. W. Cahn and J. E. Hilliard, J. Chem. Phys. **31**, 668 (1959).
[14] J. W. Cahn, Trans. Metall. Soc. AIME **242**, 166 (1968).
[15] J. E. Hilliard, in *Phase Transformations*, edited by H. L. Anderson (American Society for Metals, Metals Park, OH 1970).
[16] G. W. Smith and N. A. Vaz, Liq. Cryst. **3**, 543 (1988).
[17] G. W. Smith, Mol. Cryst. Liq. Cryst. B **180**, 201 (1990).
[18] G. W. Smith, G. M. Ventouris, and J. L. West, Mol. Cryst. Liq. Cryst. **213**, 11 (1992).
[19] G. W. Smith, Mol. Cryst. Liq. Cryst. **225**, 113 (1993).
[20] P. G. de Gennes, *Scaling Concepts in Polymer Physics* (Cornell University Press, Ithaca, 1979).
[21] J.-C. Lin and P. L. Taylor, Phys. Rev. E **49**, 2476 (1994).
[22] All PDLCs seem to have upper critical solution points [19].
[23] Y. Hirai, S. Niiyama, H. Kumai, and T. Gunjima, Rep. Res. Lab. Asahi Glass Co., Ltd. **40**, 285 (1990).
[24] Y. Hirai, S. Niiyama, H. Kumai, and T. Gunjima, Proc. SPIE **1257**, 2 (1990).
[25] A. Coniglio, H. E. Stanley, and W. Klein, Phys. Rev. Lett. **42**, 518 (1979).
[26] A. Coniglio, H. E. Stanley, and W. Klein, *Phys. Rev. B* **25**, 6805 (1982).
[27] S. C. Glotzer, M. F. Gyure, F. Sciortino, A. Coniglio, and H. E. Stanley, Phys. Rev. E **49**, 247 (1994).
[28] P. L. Taylor and R. J. Kaplar (unpublished).
[29] A. Coniglio and T. C. Lubensky, J. Phys. A **13**, 1783 (1980).
[30] F. Sciortino, R. Bansil, H. E. Stanley, and P. Alstrøm, Phys. Rev. E **47**, 4615 (1993).
[31] See, e.g., J. D. Gunton, M. San Miguel, and P. S. Sahni, in *Phase Transitions and Critical Phenomena*, edited by C. Domb and J. L. Lebowitz (Academic, London, 1983), Vol. 8, pp. 267–466.
[32] H. Tang and K. F. Freed, J. Chem. Phys. **94**, 1572 (1991).
[33] J. Lal and R. Bansil, Physica A **186**, 88 (1992).
[34] R. Bansil, J. Lal, and B. J. Carvalho, Polymer **33**, 2961 (1992).
[35] R. Ball, M. Nauenberg, and T. A. Witten, Jr., Phys. Rev. A **29**, 2017 (1984).
[36] In chemically more realistic models, the reaction would not be governed by contact of monomer molecules with the network, but with radical groups. These are either dissociated activators or activated polymer molecules, leading a more or less "ghostly" existence [H. M. J. Boots (private communication)].
[37] See, e.g., *On Growth and Form*, edited by H. E. Stanley and N. Ostrowsky (Nijhof, Dordrecht, 1985).
[38] J. M. Hyman, Physica D **12**, 396 (1984).
[39] P. I. Tamborenea and S. Das Sarma, Phys. Rev. E **48**, 2575 (1993).
[40] J. S. Langer, in *Directions in Condensed Matter Physics*, edited by G. Grinstein and G. Mazenko (World Scientific, Philadelphia, 1986), pp. 164–186.
[41] A. A. Wheeler, B. T. Murray, and R. J. Schaefer, Physica D **66**, 243 (1993).
[42] P. Keblinski, A. Maritain, F. Toigo, and J. R. Banavar, Phys. Rev. E **49**, R4795 (1994).
[43] Y. Oono and S. Puri, Phys. Rev. Lett. **58**, 836 (1987).
[44] Y. Oono and S. Puri, Phys. Rev. A **38**, 434 (1988).
[45] S. Puri and Y. Oono, Phys. Rev. A **38**, 1542 (1988).
[46] W. H. Press, S. A. Teukolsky, W. T. Vetterling, and B. P. Flannery, *Numerical Recipes: The Art of Scientific Computing*, 2nd ed. (Cambridge University Press, Cambridge, 1992).
[47] Y. Oono and Y. Shiwa, Mod. Phys. Lett. B **1**, 49 (1987).
[48] Y. Oono and M. Bahiana, Phys. Rev. Lett. **61**, 1109 (1988).
[49] M. Bahiana and Y. Oono, Phys. Rev. A **41**, 6763 (1990).
[50] H. M. J. Boots, Physica A **147**, 90 (1987).
[51] See [44,45,47–49] for the relationship between partial differential equation and CDS models.
[52] L. Leibler, Macromolecules **13**, 1602 (1980).
[53] T. Kawakatsu, Phys. Rev. E **50**, 2856 (1994).
[54] C. Sagui and R. C. Desai, Phys. Rev. E **49**, 2225 (1994).
[55] C. Sagui and R. C. Desai, Phys. Rev. Lett. **74**, 1119 (1995).
[56] F. Liu and N. Goldenfeld, Phys. Rev. A **39**, 4805 (1989).
[57] S. C. Glotzer and A. Coniglio, Phys. Rev. E **50**, 4241 (1994).
[58] Care should be exercised when extrapolating to finite n, though. A classic example is the Cahn-Hilliard equation, which exhibits multiscaling of the structure factor in the limit $n = \infty$ [A. Coniglio and M. Zanetti, Europhys. Lett. **10**, 575 (1989)], but standard scaling for any finite n [A. J. Bray and K. Humayun, Phys. Rev. Lett. **68**, 1559 (1992)].
[59] P. G. de Gennes, J. Phys. Lett. (Paris) **40**, L69 (1979).
[60] M. Daoud, J. Phys. (France) IV **3**, C1-211 (1993).

[61] B. A. Huberman, J. Chem. Phys. **65**, 2013 (1976).
[62] W. Löser and G. Vojta, Z. Phys. Chem. (Leipzig) **263**, 497 (1982).
[63] S. C. Glotzer, E. A. Di Marzio, and M. Muthukumar, Phys. Rev. Lett. **74**, 2034 (1995).
[64] See, e.g., D. Stauffer, *Introduction to Percolation Theory* (Taylor & Francis, London, 1985), p. 17.
[65] This is indeed seen in our model, for $\psi_0 \sim 0.2$–0.3.
[66] L. Ramírez-Piscina, A. Hernandéz-Machado, and J. M. Sancho, Phys. Rev. B **48**, 119 (1993).
[67] J. S. Langer, in *Solids Far From Equilibrium*, edited by C. Godrèche (Cambridge University Press, Cambridge, 1992), pp. 297–363.
[68] H. Tomita, Prog. Theor. Phys. **85**, 47 (1991).
[69] A. Shinozaki and Y. Oono, Phys. Rev. E **48**, 2622 (1993).
[70] P. I. C. Teixeira and B. M. Mulder (unpublished).
[71] U. Frisch, B. Hasslacher, and Y. Pomeau, Phys. Rev. Lett. **56**, 1505 (1986).
[72] G. R. McNamara and G. Zanetti, Phys. Rev. Lett. **61**, 2332 (1988).

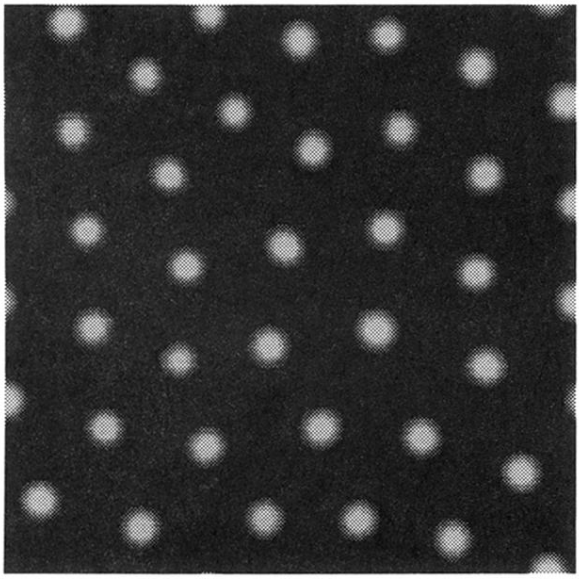

FIG. 10. Same as Fig. 7, but at $t = 50\,000$.

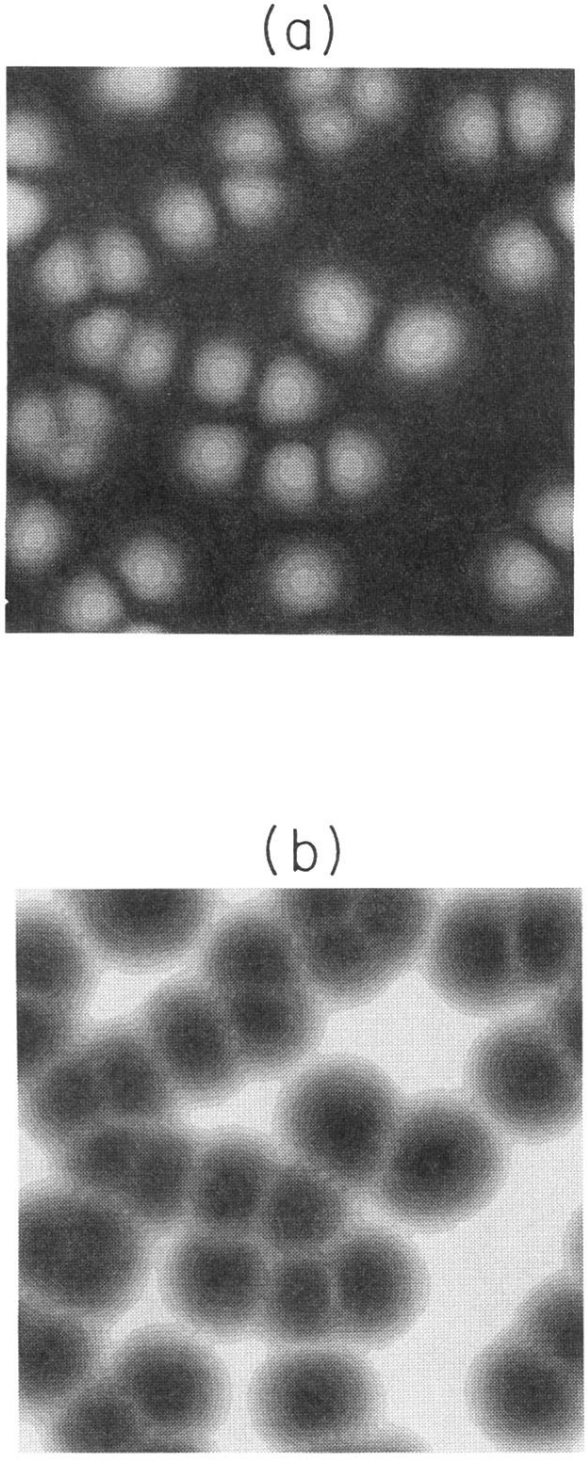

FIG. 4. (a) Monomer and (b) gel concentrations for the same system as in Fig. 3, but at $t = 10$.

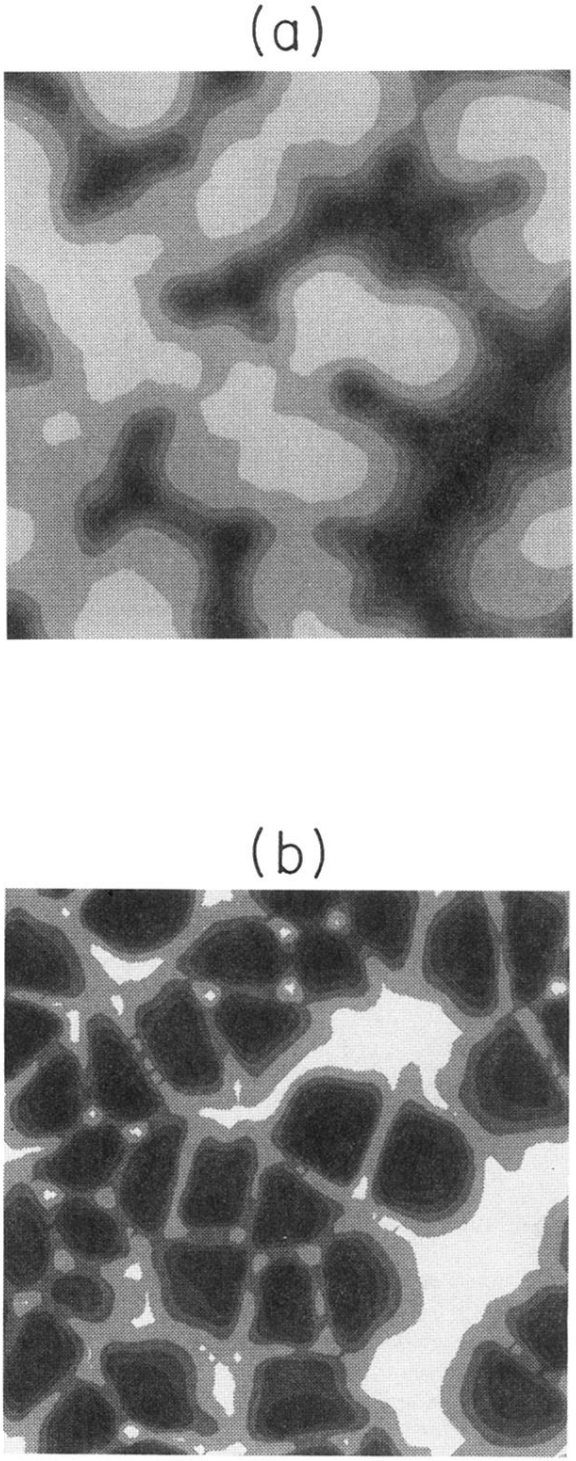

FIG. 5. Same as Fig. 4, but at $t = 50$.

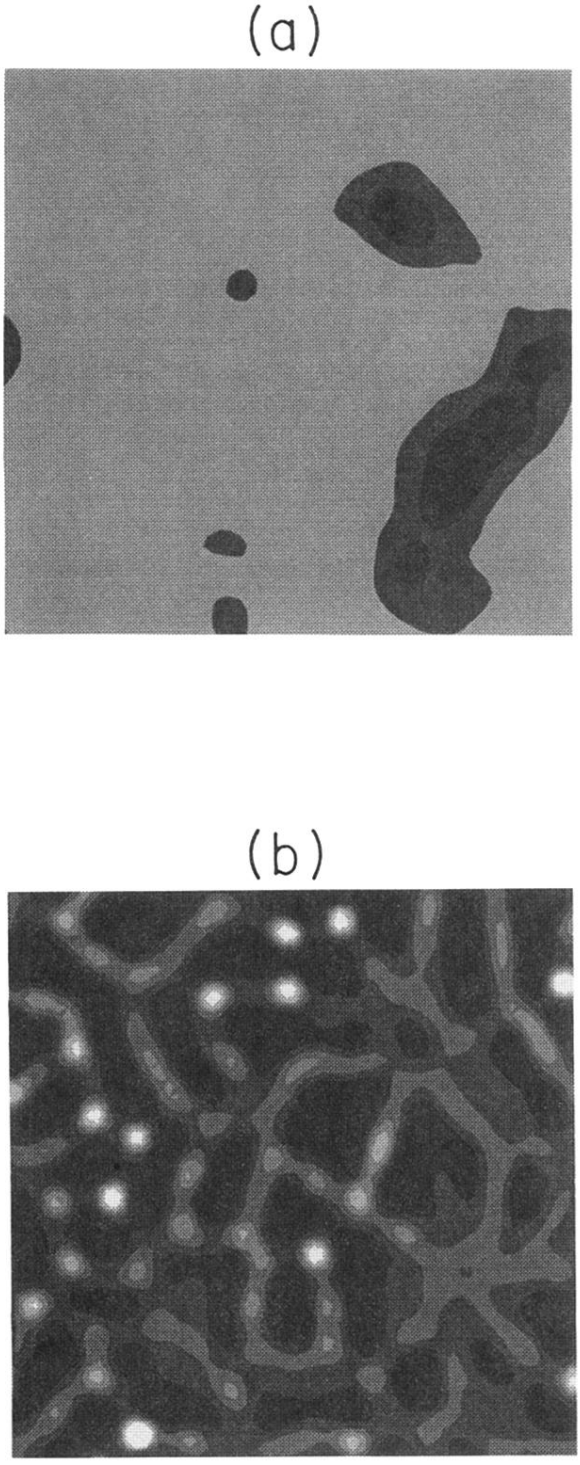

FIG. 6. Same as Fig. 4, but at $t = 100$.

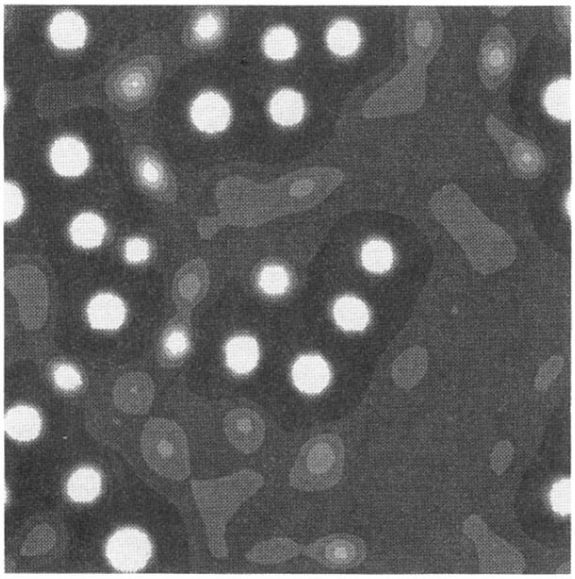

FIG. 7. Gel concentration at $t = 250$, for the same system as in the preceding figures.

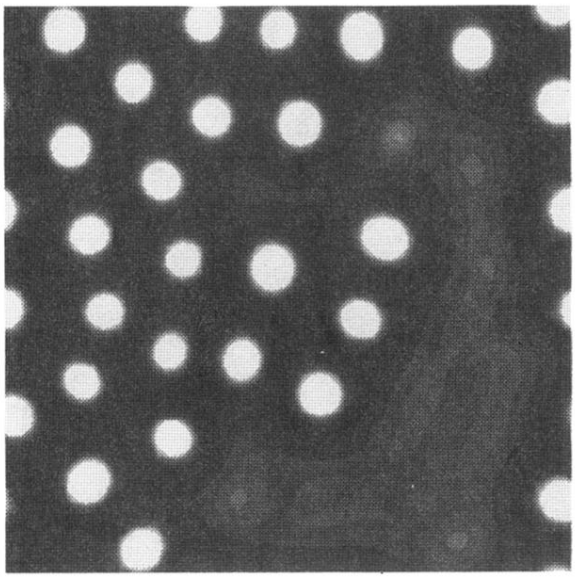

FIG. 8. Same as Fig. 7, but at $t = 1000$.

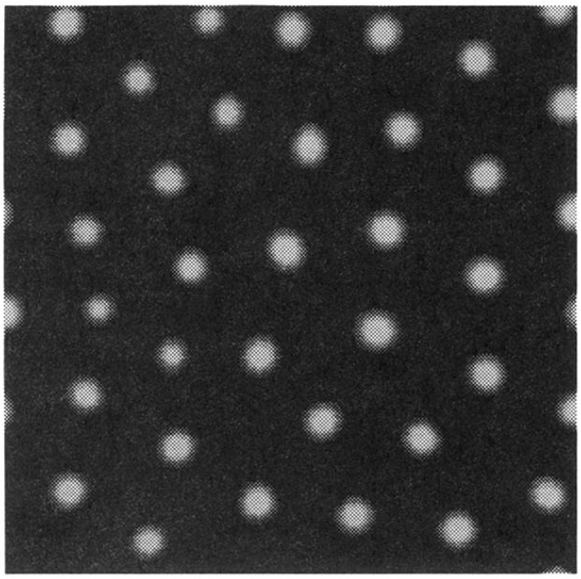

FIG. 9. Same as Fig. 7, but at $t = 5000$.